Selective clay placement within a silicate clay- epoxy blend nanocomposite and the effect on physical properties

Sandi G. Miller[1*], Daniel A. Scheiman[2], Lee W. Kohlmman[3]

[1]*Polymers Branch, NASA Glenn Research Center*

Cleveland, OH 44135

[2]*ASRL, Cleveland, OH 44135*

[3]*Department of Civil Engineering, The University of Akron, Akron, OH 44325*

**Corresponding Author: ph 216-433-8489, fax: 216-977-7132,*

e-mail: Sandi.G.Miller@nasa.gov

Abstract

Many epoxy systems under consideration for composite pressure vessels are composed of toughened epoxy resins. In this work, epoxy blends containing both rigid aromatic and flexible aliphatic components were prepared, to model toughened systems, and determine the optimum route of silicate addition. Compositions were chosen such that both glassy and rubbery resins were obtained at room temperature. The physical properties of the nanocomposites varied with T_g and silicate placement, however, nanocomposite T_gs were observed which exceeded that of the base resin by greater than 10^{o}C. The tensile strength of the glassy resin remained constant or decreased on the dispersion of clay while that of the rubbery material doubled. Selectively placing the clay in the aliphatic component of the rubbery blend resulted in a greater than 100% increase in material toughness.

Keywords: Polymer Science and Technology, Polymer Composite Materials

1. Introduction

Dispersing layered silicate clay into a polymeric matrix may influence different matrix properties in vastly differing manners; especially with regard to mechanical properties. Factors influencing the variation in mechanical performance may include: resin properties, silicate loading, degree of silicate dispersion, and the chemistry of the organic modifier on the clay.[1-3] For example, trade-offs in material properties have been

observed, such as an increase in strength and modulus leading to reduced ductility and toughness.[4] Several researchers have noted that this trend does not hold when a tensile load is applied at a temperature above the nanocomposite T_g. Pinnavaia et al.[5-6] noted that silicate dispersion into flexible resin systems, with a low T_g, results in enhancements to the material strength that greatly exceed those resulting from clay addition to a more rigid, glassy matrix. Giannelis et al.[7-8] provided evidence that clay mobility in the matrix allowed for layer orientation, thereby providing a mechanism for energy dissipation and strengthening of the material. Similarly, studies have shown an increase in the nanocomposite toughness of high T_g epoxies blended with rubber tougheners that far exceeds that of the untoughened nanocomposites.[9-10]

The synergism observed in nanocomposites prepared with a toughened polymer matrix was the interest of this study. Such synergy may result from the improved silicate mobility, as stated above, as well as a strengthening of the mechanically weaker toughening phase. In this work, the influence of silicate mobility on the nanocomposite tensile properties was addressed by tuning the T_g of the matrix resin through variation of the aromatic content in the blend. This blend approach allowed preparation of matrices, composed of identical monomers, that were either rubbery or glassy at room temperature.

Nanocomposites prepared by simply mixing the clay into the above described blends offered insight into the influence of matrix mobility. It was also of interest to evaluate the effect that strengthening the mechanically weaker toughening phase exhibited on the material properties. Therefore, we report on the mechanical properties of nanocomposites where the clay was placed within the “toughening” component of the blend. Such placement optimized the mobility of the clay, as well as reinforced the mechanically weaker component of the blend. This was achieved by pre-swelling the clay in the aliphatic component.

Studies reported in the literature[11-13] are beginning to show a preference of clay for aromatic (over aliphatic) components of block copolymers, however, there are no studies in which a pre-swelling technique was used to direct placement of the clay. Placing the clay in a specific part of the blend through physical, rather than chemical, contacts is a valid approach to force less desirable interactions. The pre-swelling approach offers the

potential for improved dispersion, as has been demonstrated by researchers who have used this technique in the past.[14-17]

In many toughened epoxy systems, the more mobile region is the rubber toughener. In this study, a reactive diluent was used for toughening. Pre-swelling organically modified clay in the flexible, aliphatic monomer, forced the clay to reside in the mobile regions of the blend. As this was also the mechanically weaker and lower modulus components of the blend, such manipulation optimized the benefits of the clay and resulted in significant enhancements to both epoxy strength and toughness.

2. Experimental

2.1 Materials

Epoxy resin, Epon 826, was supplied by Resolution Performance Products. Araldite DY3601, a polypropylene oxide based epoxide, and Jeffamine D230 curing agent were supplied by Huntsman Chemicals. The organically modified clay, Cloisite 30B, was supplied by Southern Clay Products. The structures of Epon 826, DY3601, D230, and the organic modification of Cloisite 30B are shown respectively in Figure 1.

2.2 Nanocomposite Preparation

Resin plaques of Epon 826 (aromatic) and DY3601 (aliphatic) epoxy blends were prepared in 90:10, 70:30, and 50:50 equivalent epoxy ratios; with the first number corresponding to the EPON 826 content, and the second number referring to the DY3601 content.

Resin plaque preparation at a 70:30 ratio required mixing Epon 826 (18.4 g) and DY3601 (7.875g) in a jar, followed by stirring 40^{o}C. Either 2 wt% or 5 wt% of Cloisite 30B was added and the mixture was stirred with a stir bar for 3 hours. The epoxy/clay mixture was cooled and the D230 curing agent (7.5 g) was added. The contents of the jar were poured into a 10.2 cm by 10.2 cm mold, degassed at 40^{o}C for 3 hours, then cured at 75^{o}C for 2 hours and 125^{o}C for 2 hours.

The above procedure was followed for all sample ratios prepared. The monomer quantities varied as follows: Plaques with a 50:50 blend of the epoxy resins were prepared, using Epon 826 (13.52g), DY3601 (13.52g), and D230 (6.75g), and the 90:10 ratio plaques contained: Epon 826 (22.95g), DY3601 (2.55g), and D230 (8.25g).

Resin plaques containing pre-swollen clay were prepared by sonicating 2 wt% or 5 wt% 30B, where clay concentrations were based on the final nanocomposite weight, with 5% or 10%, respectively, DY3601 epoxy resin. The clay and epoxy mixture was sonicated for 2 hours to allow for intercalation into the clay galleries. Following sonication, the swollen clay was added to EPON 826 and any additional DY3601 that would be required. The mixture was stirred with a stir bar for 3 hours, allowed to cool, and the calculated quantity of D230 curing agent was added. The mixture was poured into a 10.2 cm by 10.2 cm mold and degassed at 40°C for 3 hours then cured at 75°C for 2 hours and 125°C for 2 hr.

Epon 826

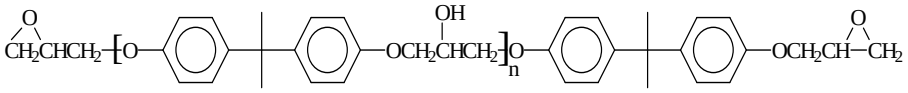

Mn ≤700, n~1

DY3601

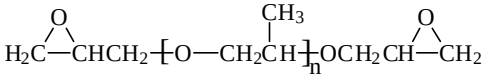

Mn < 385

Jeffamine D230

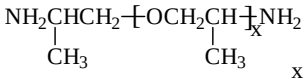

x = 2.6

Cloisite 30B Modifier

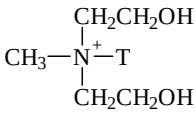

Where T is Tallow (~65% C18, ~30% C16, and ~5% C14

Figure 1. Chemical structures of Epon 826, Araldite DY3601, Jeffamine D230, and the organic modifier on Cloisite 30B

2.3 Characterization

X-ray diffraction (XRD) patterns were obtained using a Philips XRG 3100 X-ray diffractometer with Ni-filtered CuKα radiation with the XRD data was recorded in the range of $2\theta = 2^{o}$ to 32^{o}. An increase in the basal layer spacing, which was determined from a shift in the (001) peak position, indicated monomer or polymer intercalation

between the silicate layers. Disappearance of the (001) peak suggested an exfoliated morphology.

Transmission electron microscopy (TEM) specimens were prepared by microtoming nanocomposite samples, 20 to 70 nm thick, and floating the sections onto Cu grids. Micrographs were obtained with a Philips CM 200, using an acceleration voltage of 200 kV. The TEM images shown throughout this work are representative of the dispersion observed throughout several sections, taken from various regions, of each nanocomposite sample.

A Perkin Elmer High Pressure Differential Scanning Calorimeter (HP- DSC) was used to determine T_g of the epoxy samples. The resin (8-12 mg) was weighed into a sealed aluminum DSC pan. The tests were performed at 200 psi under nitrogen and the temperature was ramped from -50^{o}C to 250^{o}C at a rate of 10^{o}C/min.

Tensile tests were run according to ASTM D638. The tests were performed on MTS 800 instrument at a displacement rate of 0.55 inch per minute, using a 500 pound load cell. Optical measurement techniques using digital image correlation, as opposed to strain gages, were made using ARAMIS software. In image correlation, a random speckle pattern is painted on to the specimen. Cameras then track the displacements of the speckled dots, and displacement fields and strains are calculated by specialized computer algorithms. Once calibrated, the software can measure specimens under loading and output strain and displacement results through automated methods without user intervention being required.[18]

3. Results

3.1 Characterization of silicate dispersion

Representative XRD patterns are shown in Figures 2a-c. The XRD pattern of Cloisite 30B displayed an intense diffraction peak at $2\theta = 4.9^o$, $d_{001} = 1.8$ nm. Within the 50:50 nanocomposites, the XRD pattern suggested exfoliation, based on the absence of a Cloisite 30B diffraction peak. As the content of the aliphatic component within the epoxy blend decreased, intercalation became the prevalent nanostructure. For example, the 70:30 resin containing 5 wt% Cloisite 30B and both 90:10 nanocomposites exhibited

a low intensity diffraction peak at $2\theta = 2.51^{o}$, $d_{001} = 3.5$ nm, corresponding to intercalated clay.

In addition to XRD, TEM was employed to identify the nature of silicate dispersion within each blend composition. Representative TEM images, Figures 3a-c, indicated mixed nanocomposite morphologies; where samples contained regions of both intercalated and exfoliated silicate layers.

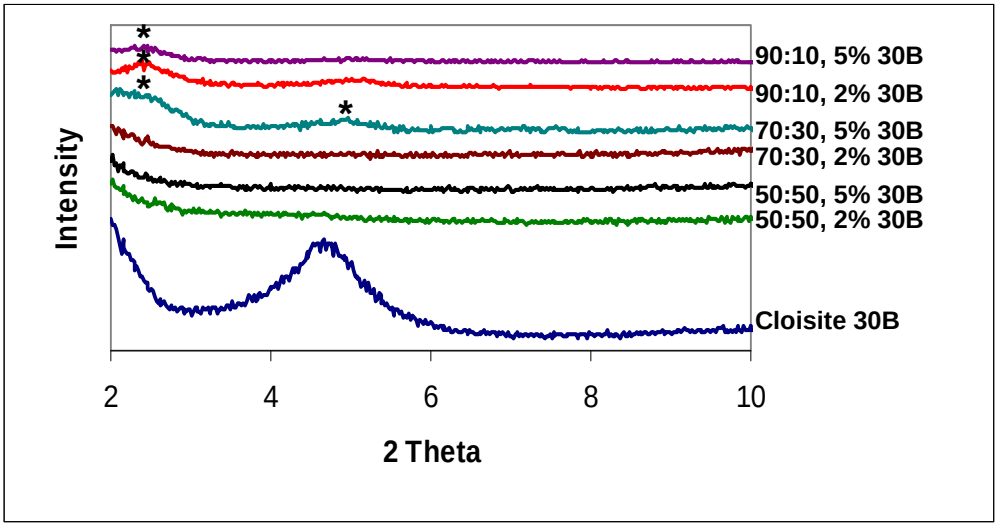

Figure 2: XRD patterns of 90:10, 70:30, and 50:50 nanocomposites.

(a)

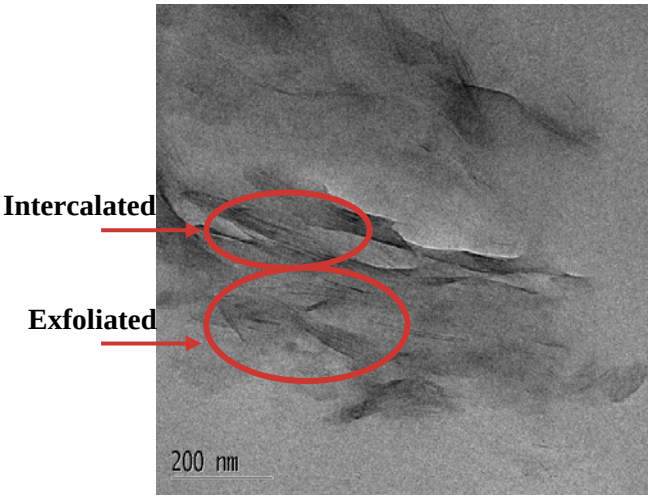

(b)

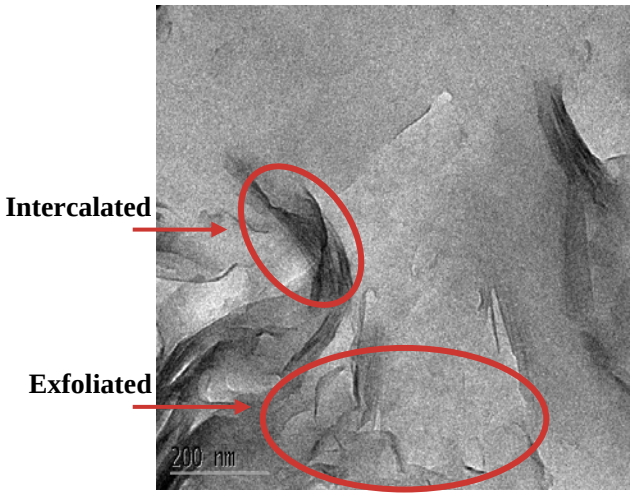

(c)

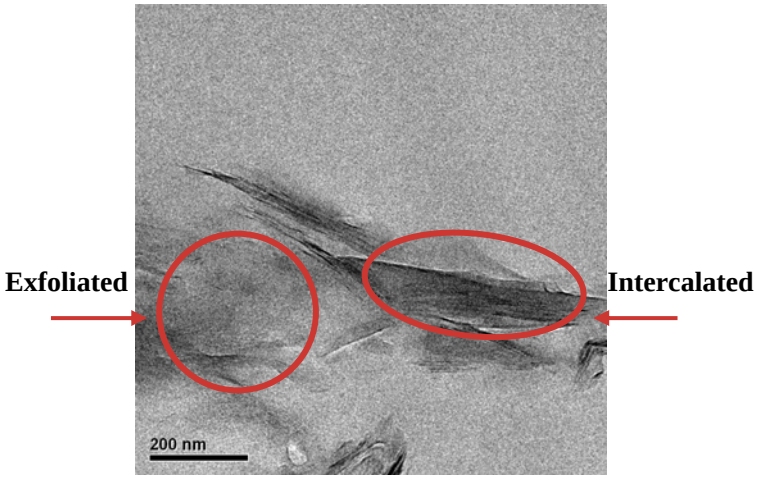

Figure 3.(a-b) Representative TEM images of 2 wt% and 5 wt% 30B, respectively, in 70:30 systems. (c) illustrates dispersion of 2 wt% 30B in 90:10 resin

Placing the silicate in contact with the flexible, aliphatic component of the blend (DY3601), was accomplished by pre-swelling the clay with that material. The XRD pattern of the pre-swollen clay, Figure 4, showed two diffraction peaks. The peak at $2\theta = 4.8^{o}$, $d_{001} = 1.7$ nm, corresponded to the unswollen Cloisite 30B. Following intercalation of the aliphatic component of the blend, the peak intensity decreased by approximately 50% and a second diffraction peak appeared at $2\theta = 2.4^{o}$, $d_{001} = 3.4$ nm, corresponding to

clay layers intercalated with the aliphatic component. The TEM images in Figures 5a and 5b demonstrate that the pre-swelling process yielded a degree of layer separation that was comparable to, if not greater than, those prepared by simply mixing all the epoxy components.

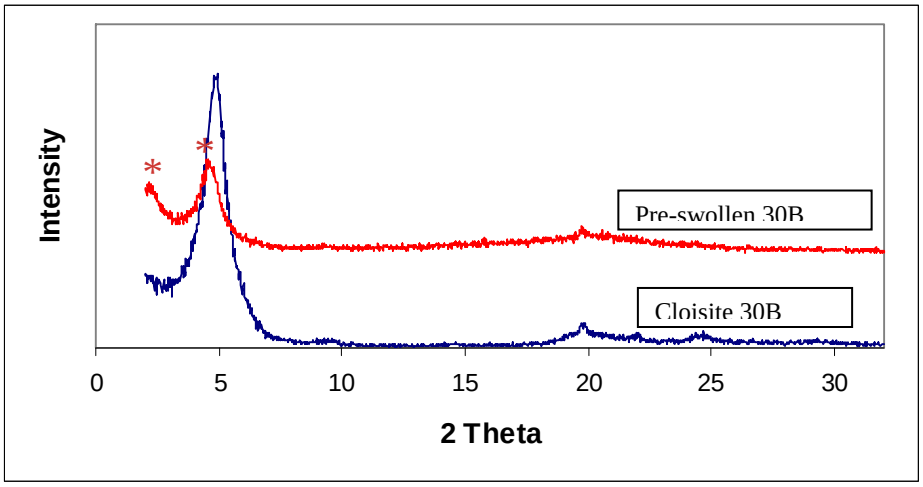

Figure 4. XRD pattern of Cloisite 30B and 2% 30B pre-swollen in DY3601

a) 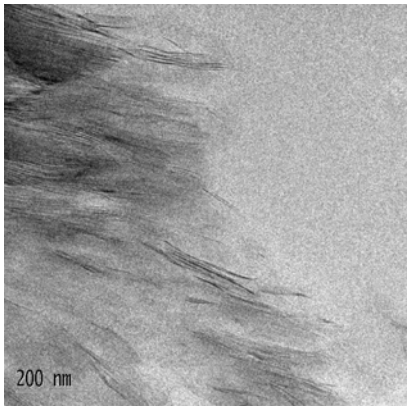

(b) 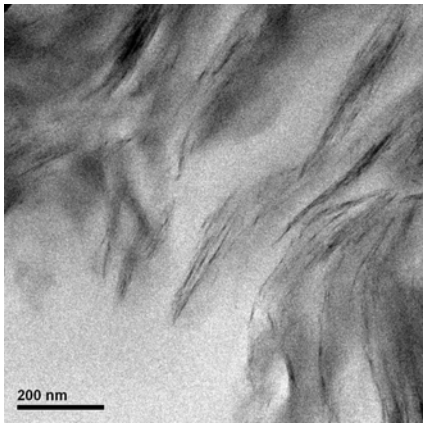

Figure 5 (a-b) Representative TEM images of 2% 30B in 70:30 epoxy matrix prepared by (a) simple mixing, and (b) pre-swelling the clay layers

3.2 Glass Transition Temperature

Resin and nanocomposite T_g values are listed in Table 1. The blend compositions with greater aromatic content generally resulted in a higher T_g. The clay offered little or no influence on the T_g of the 90:10 or the 50:50 series of resins. Within the 70:30 resins,

however, pre-swelling Cloisite 30B in the aliphatic component had a dramatic effect on T_g. Pre-swelling 2 wt% clay in the aliphatic component increased T_g above that of the base resin by 9°C. The same trend was observed at 5 wt% loading; increasing T_g by 13°C.

Table 1. T_g Measurements by DSC

Clay Content	**T_g (°C) 90:10**	**T_g (°C) 70:30**	**T_g (°C) 50:50**
0% clay	63 $^{+}$/- 2	32 $^{+}$/- 2	0 $^{+}$/- 1
2% 30B	62 $^{+}$/- 2	29 $^{+}$/- 1	-1 $^{+}$/- 2
2% 30B (pre-swollen)	67*	41*	0*
5% 30B	66 $^{+}$/- 1	30 $^{+}$/- 8	-2 $^{+}$/- 2
5% 30B (pre-swollen)	65*	45*	0 $^{+}$/- 3

* Data from one sample

3.3 Tensile Tests

The yield stress (σ_y), Young's modulus (E), and toughness of the silicate-epoxy nanocomposites were determined from stress strain curves, plotted following tensile tests. Sample plots are illustrated in Figures 6a and 6b, and the data from each plot is listed in Table 2.

3.3.1 General trends observed from tensile testing

In general, resin modulus increased with either increased aromatic content or increased clay content. An additional increase in modulus was observed following pre-swelling the clay with the aliphatic component of the blend. The yield stress also increased with increased aromatic or clay content; again with greater values of strength attained by pre-swelling. The exception was within the 90:10 series, where the nanocomposites did not yield, therefore, the reported σ_y is actually the stress at failure.

Table 2. Yield stress as determined from tensile tests

Clay Content	σ_y (psi)			E (psi)			Toughness (psi)		
	90:10*	**70:30**	**50:50***	**90:10**	**70:30**	**50:50**	**90:10**	**70:30**	**50:50**
0% clay	9741 +/- 200	2568 +/- 6	189 +/- 21	4509 +/- 57	1124 +/- 53	9 +/- 1	1110 +/- 200	1270 +/- 90	34 +/- 3
2% 30B	9549 +/- 170	2281 +/- 71	270 +/- 13	4504 +/- 1	997 +/- 179	11 +/- 1	190 +/- 20	1020 +/- 40	31 +/- 3
2% 30B (pre-swollen)	8770**	3673 +/- 198	328 +/- 5	4701**	1640 +/- 162	13 +/- 2	100**	1430 +/- 110	74 +/- 5
5% 30B	8355 +/- 221	3324 +/- 31	352 +/- 16	4762 +/- 70	1575 +/- 147	12 +/- 2	120 +/- 20	1450 +/- 40	39 +/- 4
5% 30B (pre-swollen)	7690 +/- 451	4193 +/- 129	365 +/- 5	4687 +/- 98	2023 +/- 182	15 +/- 1	90 +/- 10	990 +/- 150	79 +/- 10

* Stress at failure.

** Data from one sample due to air bubbles within the material.

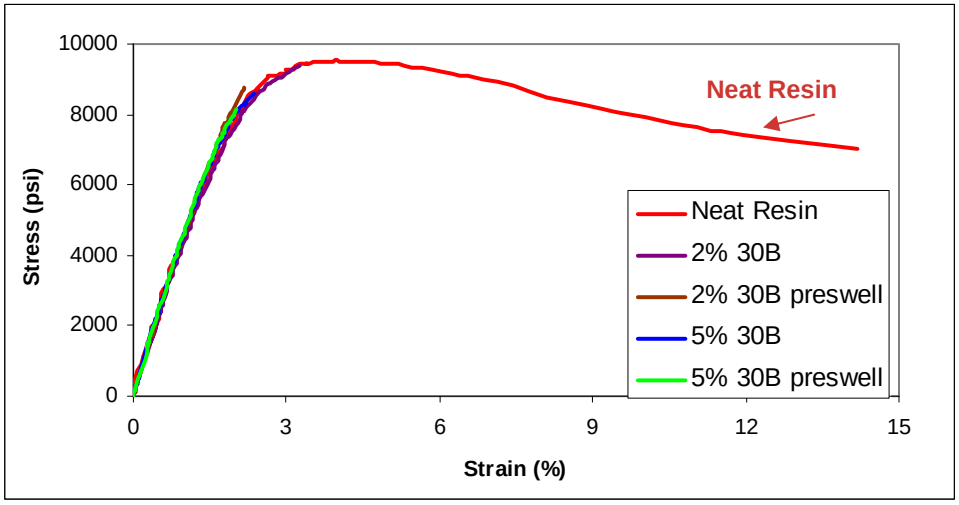

(a)

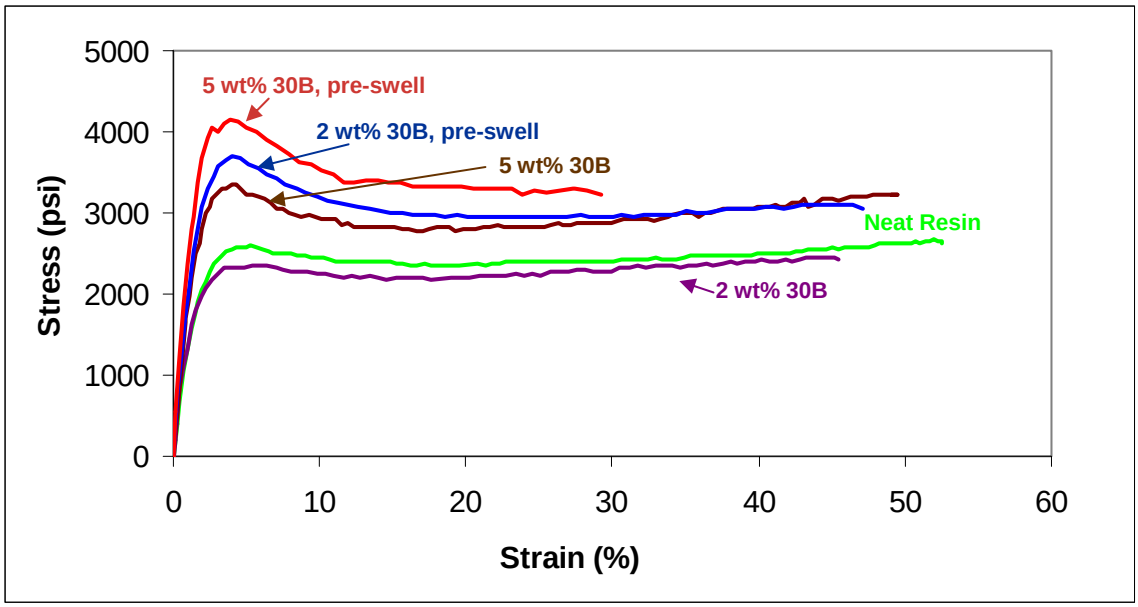

(b)

Figures 6(a-b) Stress – Strain curves of 90:10 and 70:30 series, respectively

As the nanocomposites failed earlier than the neat resin, the reported σ_y of the nanocomposites was lower than that of the base resin.

Within the glassy specimens (70:30 and 90:10), the increase in E and σ_y was accompanied by a reduced or unchanged value calculated for toughness. However in the 50:50 series, which was rubbery at room temperature, the nanocomposite toughness was increased despite the increase of strength and modulus.

4. Discussion

4.1 Interaction between Cloisite 30B and aromatic or aliphatic compounds

The interaction between the silicate clay and an aromatic or aliphatic compound was evaluated by the addition of 0.5 g Cloisite 30B to 20mL of either chlorobenzene or hexanes. Following addition to hexanes, the clay remained in powder form and immediately settled to the bottom of the solution. However, mixing Cloisite 30B with chlorobenzene resulted in instantaneous swelling and dispersion of the clay throughout the solvent, as pictured in Figure 7. The swelling indicated a much greater attraction

between the aromatic compound and the silicate clay and was consistent with SANS data that has been reported in the literature.[14]

The observation that Cloisite 30B had an affinity for aromatic containing compounds suggested that, within the epoxy blend nanocomposite, the clay may have resided in closer contact with the more rigid, aromatic component of the epoxy blend. This would leave the more flexible, and mechanically weaker, aliphatic component with minimal silicate reinforcement.

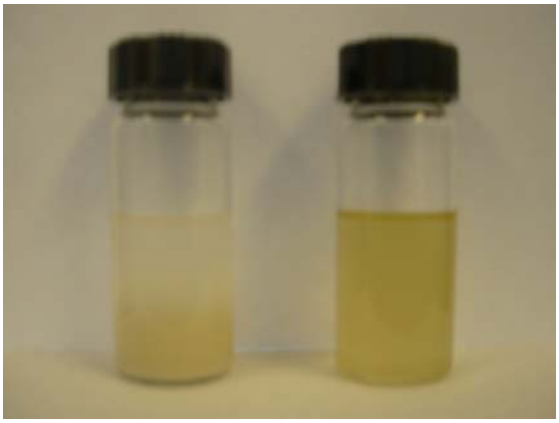

Figure 7. Cloisite 30B aggregates in hexanes (left) and dispersed in chlorobenzene (right)

4.2. Microstructure

The single T_g reported within each system indicated a miscible system. Correspondingly, macrophase separation within these blends was not observed by SEM. However, the results collected did suggest a level of phase separation, which allowed for manipulation of the material properties. For example, the 70:30 blend contained 2.3 times, by weight, the amount of aromatic component over aliphatic; (2x by volume). While the rubbery component was likely well integrated into the blend, there would remain large regions composed solely of the aromatic component. As such, an affinity between the silicate and the aromatic segment which pulled the clay into these regions would render the rubbery component deficient in clay content. The SEM image in Figure 8 shows distinct regions of the 70:30 blend containing significant quantities of clay, while adjacent regions of the blend contain little visible filler.

The 50:50 series contained nearly equal quantities of both aromatic and aliphatic components. In this case, SEM images Figure 9, showed much greater homogeneity in

the silicate separation, relative to the 70:30 blend. The disparity in silicate distribution within these systems had significant influence in the nanocomposite properties, and allowed manipulation of those properties by selectively placing the clay in the aliphatic region.

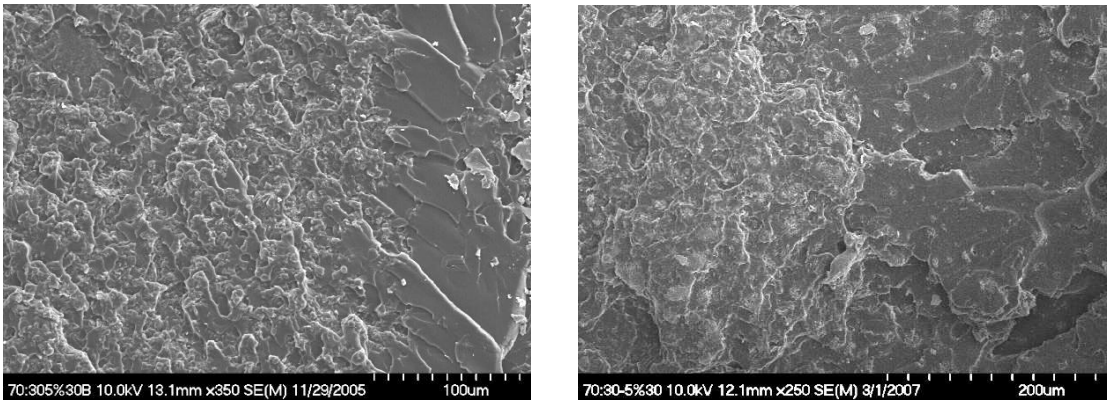

Figure 8. Representative SEM images of the fracture surface of the 70:30 resin containing 5 wt% 30B

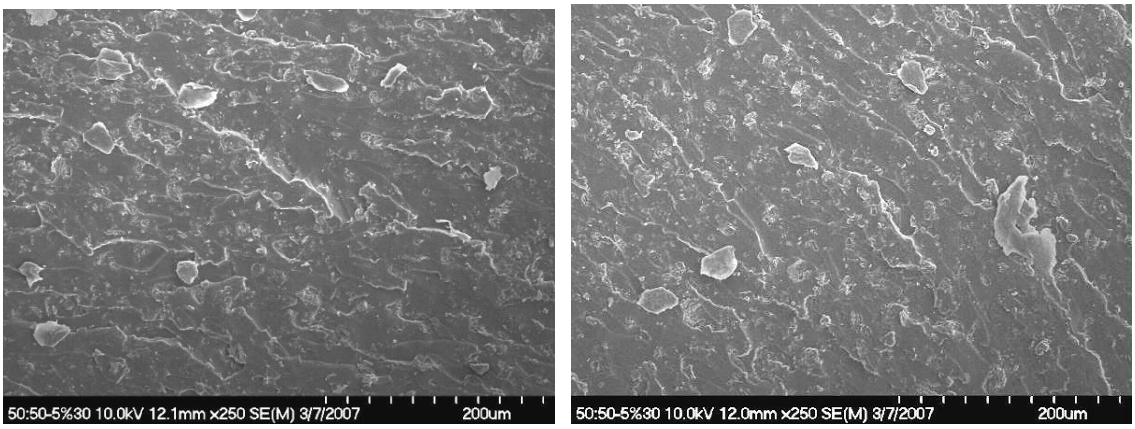

Figure 9. Representative SEM images of fracture surface of 50:50 resin containing 5 wt% 30B.

4.3 Glass Transition Temperature

It was observed that the T_g generally dropped following simple mixing of Cloisite 30B into the epoxy blends. There are two primary factors which can affect the T_g of thermosetting nanocomposites. The first is potential matrix plasticization due to the aliphatic organic modifier on the clay.[19] The second is any reduction in the crosslink

density which may occur due to the presence of the clay. Both scenarios are plausible contributors to the observed drop in T_g with silicate dispersion.

The effect of pre-swelling the clay in the rubbery component was to recover the initial T_g drop due to the presence of the clay. Pre-swelling forced the clay into the more mobile component, thus reinforcing the regions that would contribute to overall lower T_g. In the case of the 70:30 blends, pre-swelling pushed the T_g higher than that of the base resin, and an overall increase of up to 13^{o}C was observed.

4.4 Mechanical Properties

Significant benefit from pre-swelling was observed within the mechanical property data. In this case, positioning the silicate reinforcement within the flexible component allowed improved mobility of the clay, translating into improved composite strength and modulus.

The literature reports that improving the mobility of nanoclay within the matrix can enhance the toughness of the nanocomposite material as compared to the base resin.[20-24] In this study both rubbery and glassy samples were prepared. The 50:50 samples, rubbery at room temperature, showed improved toughness only following pre-swelling the clay in the more mobile component. In this case, the clay reinforced the more flexible regions of the blend, resulting in a more than 100% increase in the calculated toughness, as well as an overall stronger and stiffer composite. The enhancement to yield stress and modulus was pronounced in this material, where σ_y increased up to 93% and E up to 67%. It should be noted that the 50:50 resins also did not yield, therefore the yield stress represented the stress at failure. This is increased in all the nanocomposite samples, relative to the neat resin.

Selectively placing the clay in the more mobile component was also a significant benefit to the yield stress and modulus of most 70:30 resins. The values of both properties were further enhanced on strengthening the flexible portion of the resin blend. Addition of 2 wt% pre-swollen clay increased σ_y over 40% without a corresponding decrease in toughness, relative to the base resin. Addition of 5 wt% pre-swollen clay increased σ_y and E by 63% and 80% respectively; again without a significant change in the material toughness.

The least dramatic influence was observed with the 90:10 resins. In this case, pre-swelling the clay had no effect on the overall properties. This may be attributed to the already small concentration of flexible component present in the system. Additionally, as with the 50:50 resins, this system does not yield. Therefore, the σ_y values of the nanocomposites in the 90:10 series are reduced relative to the base resin because these nanocomposites fail earlier than the base resin.

Generally speaking, the clay benefited the mechanically weaker, rubbery regions to a greater extent than the more rigid materials, in terms of strength, modulus, and toughness. Likewise, directing the clay into the more flexible component of a blend had a similar result, and the overall properties of blend properties were improved. Therefore, pre-swelling offered the greatest benefit in mechanical properties to systems which were initially rubbery, or mechanically weaker than a similar glassy system. As the T_g increased, and the material was strengthened by its chemical structure, the clay offered less benefit than the rubbery systems, but still provided significant property enhancements. This data will be useful in designing toughened epoxy systems for any number of applications.

5. Conclusions

The observed preference of Cloisite 30B for aromatic containing compounds over aliphatic enabled preferential placement of the clay within the flexible regions of an epoxy blend. This placement was achieved by pre-swelling the clay in the aliphatic component of the blend prior to addition of the aromatic component.

Evidence that the clay did reside in a specific region of the blend was provided by SEM images. Furthermore, the increase in T_g on pre-swelling the clay suggested that the clay restricted epoxy chain motion within the mobile component of the blend. Tensile test data from the epoxy blends revealed that the mobility of the silicate layers within the matrix offered improved resin toughness. This was seen by the improved toughness and significant enhancement in strength within the pre-swollen 50:50 resins, relative to other resin in the series which are glassy at room temperature.

Placing the clay in the mobile component offered additional enhancements to both strength and modulus. As the aliphatic component was also the mechanically weaker

component of the blend, the pre-swelling step provided a mechanism to reinforce the weaker component, thereby offering additional enhancements to the strength, modulus, and glass transition temperature of the epoxy nanocomposites.

6. References

1. Shi H, Lan T, Pinnavaia TJ. Chem. Mater. 1996; 8: 1584-1587.
2. Gorrasi G, Tortora M, Vittoria V, Pollet E, Lepoittevin B, Alexandre M, Dubois P. Polymer 2003; 44: 2271-2279.
3. Chang JH, An YU. J. Polym. Sci: Part B, Polym. Phys. 2002; 40(7):670-677.
4. Becker O, Varley R, Simon G. Polymer 2002; 43: 4365-4373.
5. Wang MS, Pinnavaia TJ. Chem. Mater. 1994; 6(4): 468-474.
6. Lan T, Pinnavaia TJ. Chem. Mater. 1994; 6(12): 2216-2219.
7. Shah D, Maiti P, Jiang DD, Batt CA, Giannelis EP. Adv. Mater. 2005; 17(5): 525-528.
8. Shah D, Maiti P, Gunn E, Schmidt DF, Jiang DD, Batt CA, Giannelis EP. Adv. Mater. 2004; 16(14): 1173-1177.
9. Liu W, Hoa SV, Pugh M, Polym. Eng. Sci. 2004; 44(6): 1178.
10. Balakrishnan S, Raghavan D. Macromol. Rapid Commun. 2004; 25: 481.
11. Chastek TT, Stein A, Macosko C. Polymer 2005; 46(12): 4431.
12. Korley LT, Liff SM, Kumar N, McKinley GH, Hammond PT. Macromolecules 2006; 39: 7030-7036.
13. SANS paper
14. Usuki A, Kojima Y, Kawasumi M, Okada A, Fukushima Y, Kurauchi T, Kamigaito O. J. Mater. Res. 1993; 8: 1179-1184.
15. Jiankun L, Yucai K, Zongneng Q, Xiao-su Y. J. Polym. Sci: Part B, Polym. Phys. 2001; 39: 115-120.
16. Yang K, Ozisik R. Polymer 2006; 47: 2849-2855.
17. Ishida H, Campbell S, Blackwell J. Chem. Mater. 2000; 12: 1260-1267.
18. Littell JD, Ruggeri CR, Goldberg RK, Roberts GD, Arnold WA, Binienda WK. J. Aerospace Engineering 2008; In Publication.
19. Park J, Jana SC. Macromolecules 2003; 36(22): 8391-8397.

20. Balakrishnan S, Start PR, Raghavan D, Hudson SD. Polymer 2005; 46(25): 11255-11262.
21. Wang MS, Pinnavaia TJ. Chem. Mater. 1994; 6(4): 468-474.
22. Lan T, Pinnavaia TJ. Chem. Mater. 1994; 6(12): 2216-2219.
23. Shah D, Maiti P, Jiang DD, Batt CA, Giannelis EP. Adv. Mater. 2005; 17(5): 525-528.
24. Shah D, Maiti P, Gunn E, Schmidt DF, Jiang DD, Batt CA, Giannelis EP. Adv. Mater. 2004; 16(14): 1173-1177.